Viscoelastic Effects on Dilute Polymer Solutions Phase Demixing: Fluorescence Study of a Poly(ϵ-caprolactone) Chain in THF

Susana Piçarra and J. M. G. Martinho*

Centro de Química Física Molecular, Instituto Superior Técnico, 1049-001 Lisboa, Portugal

Received July 17, 2000; Revised Manuscript Received November 2, 2000

ABSTRACT: The demixing of a 0.002 wt % solution of a poly(ϵ-caprolactone) chain (M_w = 20 000; M_w/M_n = 1.07), labeled at both chain ends with pyrene, in tetrahydrofuran (THF) was studied using fluorescence. The very diluted region of the phase diagram of small polymer chains was explored for the first time. The coexistence curve was crossed at −30 °C, below the coil−globule transition temperature, which was observed at 0 °C. The demixing occurred from a "gas" solution of globules and small clusters, and we observed three stages before precipitation: an initial frozen stage, where particles collided but did not grow; a second region where clusters grew by incorporation of globules; and a third stage where coarsening occurred. The excimer-to-monomer fluorescence intensities ratio followed power law type dependencies in time, during both the growth and coarsening stages. This was attributed to phase demixing slowed by viscoelastic effects. The demixing was accelerated by deeper temperature quenches and retarded by slower rates of quenching.

1. Introduction

The demixing of polymer solutions is an interesting subject, and it has been studied over the past years, both theoretically and experimentally.[1−3] In a polymer−solvent phase diagram the coexistence curve (binodal line) separates a stable homogeneous phase region from a second one where two liquid phases of different polymer concentrations coexist. This equilibrium line can be reached by temperature lowering due to the decrease on the enthalpy of mixing. Nevertheless, some polymer−solvent mixtures also display an entropically induced coexistence curve for high temperatures.[4] This equilibrium line cannot be explained in the framework of regular solution thermodynamics (entropy of mixing given by the ideal combinatory entropy). The negative contribution of the entropy of mixing arises either from the dissimilarity between polymer and solvent expansion coefficients or from the presence of specific interactions between chains and solvent.[5] The maximum and minimum temperatures for phase separation are designated as upper critical solution temperature (UCST) and lower critical solution temperature (LCST), respectively. The demixing process has been studied for high molecular weight polymers and relatively concentrated solutions, using mainly light scattering[6,7] and imaging techniques.[8] At the critical composition a homogeneous solution is always unstable for temperatures lower than the UCST. Under off-critical conditions, there is a region of metastability, situated just below the coexistence curve, where a kinetic barrier for the demixing exists and phase separation occurs by a nucleation and growth (NG) mechanism.[9,10] The nucleation results from an instability, initiated by local fluctuations, that creates droplets larger than a certain critical size. These droplets, which form the minority phase, initially grow by incorporation of polymer molecules from the supersaturated solution. As the interaction among droplets is negligible, their number density is invariant in time, while the droplets' size increases. The droplet radius changes as t^{α}, α being dependent on the growth mechanism.[10] When the diffusion of the polymer chains in the supersaturated solution is the limiting step for growth, $\alpha = {}^1/_2$.[10,11] However, especially in the case of very diluted high molecular weight polymer solutions, the growth can be controlled by the polymer molecules reptation into the droplet, for which $\alpha = 1$.[11] After the growth process, a coarsening stage occurs with $\alpha = {}^1/_3$, for both evaporation−condensation (Ostwald ripening)[12] and diffusion−reaction (coalescence growth)[13] mechanisms. In this stage the number density of the droplets decreases with time while the volume fraction of the minority phase remains constant.

If temperature quench is deep enough to reach the spinodal line, which is the lowest limit of the metastable region and where the energy barrier against demixing vanishes, the unstable region is reached, and phase separation occurs spontaneously. The spinodal line coincides with coexistence curve at the critical point, lying under it on the other regions of the phase diagram. Three stages were identified in the spinodal demixing process:[7] an early stage, where loose aggregates are formed spontaneously and slowly grow in time; an intermediate stage, where growing proceeds and the solvent is discharged; and a final stage, where compact aggregates grow by a coarsening mechanism. The growth in the early stage is well described by the Cahn−Hilliard linear model,[14] developed for the spinodal decomposition of alloys and later adapted and extended to polymer blends by de Gennes,[15] Pincus,[16] and Binder.[17] In this stage domains grow very slowly while the concentration fluctuations grow exponentially. In the intermediate stage the size of the aggregates increases faster while the concentration fluctuations keep growing, until the final equilibrium concentration of the polymer-rich phase is reached. In the final stage the aggregates continue to grow in size, but there are no more fluctuations in concentration, since the equilibrium compositions of the diluted and concentrated solutions were attained. The intermediate and final stages of spinodal decomposition are rather complex and are still not completely understood.[7,8] Nevertheless, the

* To whom correspondence should be addressed. Phone 351-21 841 92 50; Fax 351-21 846 44 55; E-mail jgmartinho@ist.utl.pt.

10.1021/ma001231t CCC: $20.00
Published on Web 12/08/2000

Scheme 1

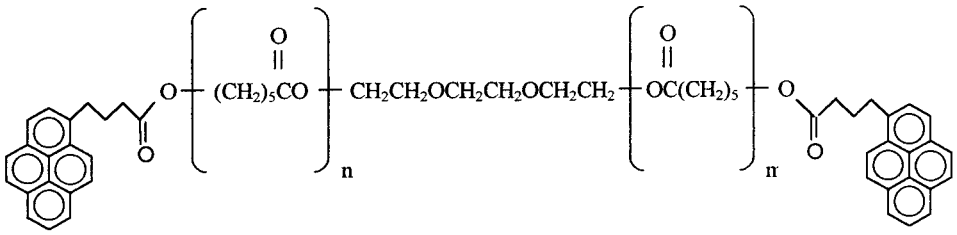

hydrodynamic flow effects discussed by Kawasaki and Ohta[18] and Siggia[19] are important when domains are interconnected, as experimentally observed[8b] and demonstrated by computer simulations.[20,21] These effects accelerate the coarsening, making the domains size scale with t^{α}, the exponent being $\alpha = 1.0$ (greater than the value predicted by both the evaporation−condensation and the diffusion−reaction mechanisms, where $\alpha = {}^1/_3$).

Most of the published studies on spinodal decomposition were performed only in critical or near-critical conditions, due to the low sensitivity of the experimental techniques. However, the study of very diluted solutions of flexible low molecular weight polymers is of great interest, since the coil−globule transition of the single chains is expected to occur much before the cross of the coexistence curve.[22] Phase demixing should then occur from a "gas" solution of globules.

The coil−globule transition temperature lies below θ_U (critical temperature for an infinite length polymer chain) and their relative separation decreases with chain stiffness, unless crystalline ordering takes place.[23] Chain stiffness determines both the characteristics of the transition (sharp or continuous) and the morphology of the globule (toroid, rod, spherical).[24] The lower the temperature, the more compact is the final equilibrium globule, as most solvent is expelled during transition.[25]

On the very diluted region of the flexible polymer chains phase diagrams, the coil−globule transition occurs above the coexistence curve. According to Allegra et al.,[26] there is no longer a distinction between the binodal and spinodal. During phase separation each globule can be considered as a critical nucleus for the demixing process. The aggregation should be controlled by the average time between globule collisions.

The collision time is given by $\tau_c = l^2/D$, where l is the range of the interaction and D is the diffusion coefficient of the globule. As D for a single globule is large, τ_c is relatively low. The time needed to establish a permanent contact between segments of two colliding chains, τ_p, is large for entangled chains in compact globules. When $\tau_p > \tau_c$, collisions are not effective, and globules behave as elastic bodies that collide many times before coalescence occurs.[27] These are named *viscoelastic effects*. Allegra et al.[26,28] showed that these particles can also be small compact clusters of chains.

To our knowledge, there are no published experimental studies dealing with the aggregation of very diluted polymer solutions of small chain polymers. This is due to the experimental difficulties associated with the low sensitivity of light scattering techniques.

In the present work we studied the aggregation of a poly(ϵ-caprolactone) chain ($M_n = 19\,200$; $M_w/M_n = 1.07$) labeled at both ends with a pyrene derivative, in THF, between −30 and −60 °C. It was recently shown by fluorescence that stable globules are formed near 0 °C, persisting in solution until around −30 °C, with no detectable formation of aggregates, during very long time periods.[29] Decreasing the temperature below −30 °C, polymer chains aggregation starts. Three distinct regions were identified on the kinetics of aggregation, and additional molecular information was obtained in all stages of phase demixing. Viscoelastic effects were found to be significant, especially in the early stage of phase demixing.

2. Experimental Section

Instrumentation. Fluorescence spectra were recorded on a SPEX Fluorolog F112A fluorimeter at several temperatures using a cryostat from Oxford Instruments (DN 1704) that allows the control of the temperature within ±0.5 °C. The fluorescence spectra were recorded between 370 and 600 nm using 330 and 360 nm excitation wavelengths.

Polymer Characterization. The synthesis of the poly(ϵ-caprolactone) terminated at both ends with OH groups and its labeling with a pyrene derivate were described by Sosnowski et al.,[30] originating the molecular structure shown in Scheme 1.

The polymer was characterized by ^{1}H NMR and by GPC as described before.[29] The $M_n = 19\,600$ calculated by NMR compares very well with the $M_n = 19\,200$ obtained by GPC. The polymer chain has a very narrow molecular weight distribution ($M_w/M_n = 1.07$) obtained by GPC. The degree of labeling calculated from the UV−vis absorption spectra, knowing M_n and the molar absorption coefficient for the methyl ester of pyrenebutyric acid in toluene at 345 nm ($\epsilon = 3.83 \times 10^4$ dm^3 mol^{-1} cm^{-1}),[31] was in close agreement with the 1.96 value found by NMR.

Sample Preparation. A 1.0×10^{-6} M (0.002 wt %) polymer solution was prepared in tetrahydrofuran (THF). THF was freshly distilled under argon and its purity verified by fluorescence at the excitation wavelengths. The solution was degassed by the freeze−pump−thaw technique (six cycles), the final pressure being better than 10^{-5} Torr. The solution was kept in the dark between measurements.

3. Results and Discussion

Figure 1 shows the fluorescence spectra of a 10^{-6} M solution (0.002 wt %) of the both-ends pyrene-labeled poly(ϵ-caprolactone) chain in THF at room temperature and 10 h after being instantaneously quenched to −30 and −40 °C.

All spectra, obtained by excitation at 360 nm, show both an intense blue band attributed to the fluorescence of pyrene monomer and dimer and a weak broad band at longer wavelengths characteristic of pyrene excimer emission. The ratio of the excimer-to-monomer fluorescence intensities, I_E/I_M, is a measure of the efficiency of excimer formation[32] and is plotted as an inset in Figure 1. The intensity ratio is practically constant between 50 and 0 °C, decreasing for lower temperatures. The decrease of the fluorescence intensity ratio results from the decrease of the rate of dimer to excimer conversion due to constrains imposed by the polymer chain in the globular state. The break point at 0 °C was identified from both steady-state and time-resolved fluorescence

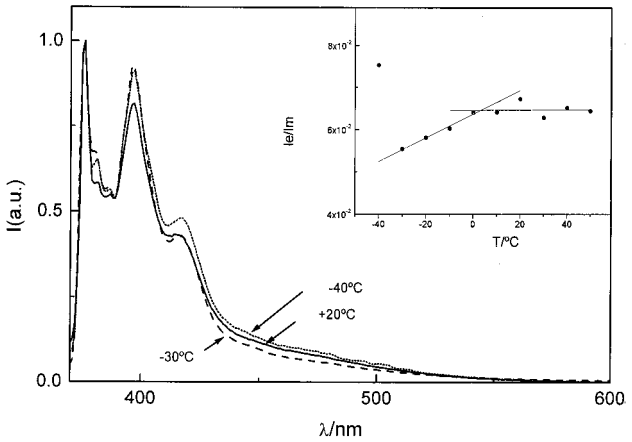

Figure 1. Fluorescence spectra of a 10^{-6} M solution of a both-ends pyrene-labeled poly(ϵ-caprolactone) chain (M_w = 19 200; M_w/M_n = 1.07) in THF by excitation at λ_{exc} = 360 nm at several temperatures: (—) 20 °C, (- - -) −30 °C; (• • •) −40 °C. All spectra were recorded 10 h after the temperature quench. Inset: ratio of the excimer at λ_{em} = 500 nm (I_E) to monomer at λ_{em} = 376 nm (I_M) fluorescence intensities as a function of quenching temperature.

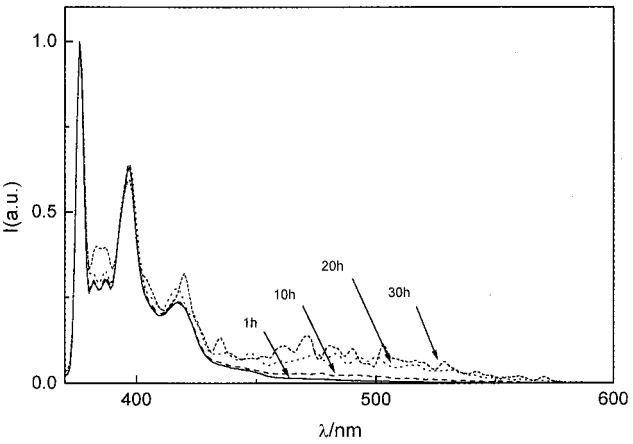

Figure 2. Fluorescence spectra of a 10^{-6} M solution of a both-ends pyrene-labeled poly(ϵ-caprolactone) chain (M_w = 19 200; M_w/M_n = 1.07) in THF at different times after being instantaneously quenched to −40 °C by excitation at λ_{exc} = 330 nm.

measurements as the coil−globule transition temperature.[29] Globules remain stable until −30 °C, as proved by the invariance of the fluorescence spectra and decay curve measurements for more than 50 h. However, slightly below −30 °C, minor changes in the fluorescence decays for very long delay times are observed, showing that globule association was initiated and that the coexistence line was crossed. At −40 °C, the relative excimer-to-monomer fluorescence intensity is considerably higher.

Figure 2 shows the fluorescence spectra of the polymer solution recorded at several times after being instantaneously quenched to −40 °C.

The relative excimer-to-monomer fluorescence intensity increases with time. As the characteristic time for coil−globule transition is of the order of minutes, these spectra changes must be attributed to aggregation that can occur at much longer times. Around 3.5 h after the temperature quench, the spectra begin to show fluctuations in both monomer and excimer emission regions. These fluctuations are a clear indication of the heterogeneity of the solution. In the very diluted region of the phase diagram it is predicted that, below the coil−

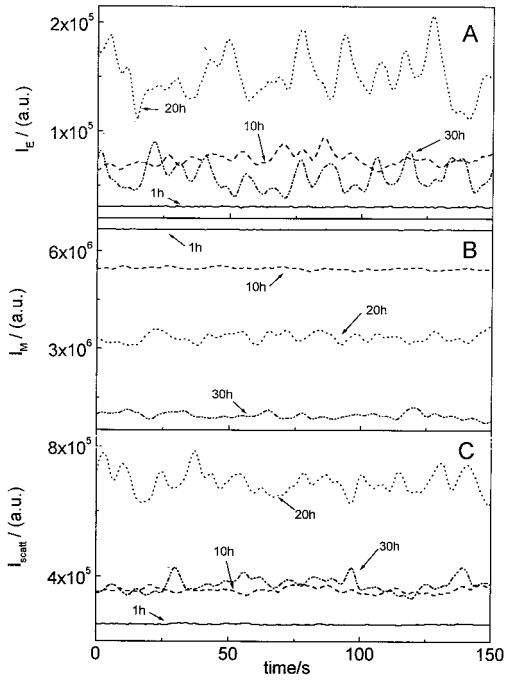

Figure 3. Intensities versus time for several times after an instantaneous quench to −40 °C: (A) excimer fluorescence (λ_{em} = 500 nm); (B) monomer fluorescence (λ_{em} = 376 nm); (C) scattered light (λ = 360 nm).

globule transition temperature, the binodal and spinodal curves will coincide. This, although not predicted by the mean-field theories, is a consequence of chain connectivity.[28] At the quenching temperature polymer coils can form either globules or aggregate, because they are simultaneously below the coil−globule transition temperature and the coexistence curve. During the globulization process some chains can collide and form small clusters. At the end, the mixture is composed of small clusters and compact equilibrium globules. In the two-phase region of the phase diagram these clusters can be considered as the constituents of the polymer-rich phase and are responsible for the demixing process. The system is still out of equilibrium and will progress to form larger aggregates, reducing the surface energy.

To study in detail these fluctuations, the monomer (λ_{em} = 376 nm) and excimer (λ_{em} = 520 nm) fluorescence as well as the scattered light (λ = 360 nm, 90° scatter angle) intensities were plotted in Figure 3 during 150 s, for several delay times after the quench to −40 °C.

The scattered light was recorded at 360 nm because the scattering is higher at shorter wavelengths, and the presence of pyrene dimers enhances the effect.[33]

Fluctuations in intensity are due to aggregates that intermittently cross the excitation beam, while the background results from small globules dispersed in the majority phase. The shape and intensity of the fluctuations indicate the presence of aggregates of several sizes. No percolation was expected to occur, as interaction between particles is very small in diluted solutions.

The lower scattering intensity at 30 h relative to 20 h is attributed to polymer precipitation (see Figure 3C).

In Figure 4 is shown a log−log plot of the excimer-to-monomer fluorescence intensity ratio, I_E/I_M, values averaged over 200 s, versus time t, for several instantaneous temperature quench depths (from room temperature).

A period of 200 s was considered enough as no changes in the average values were observed for periods

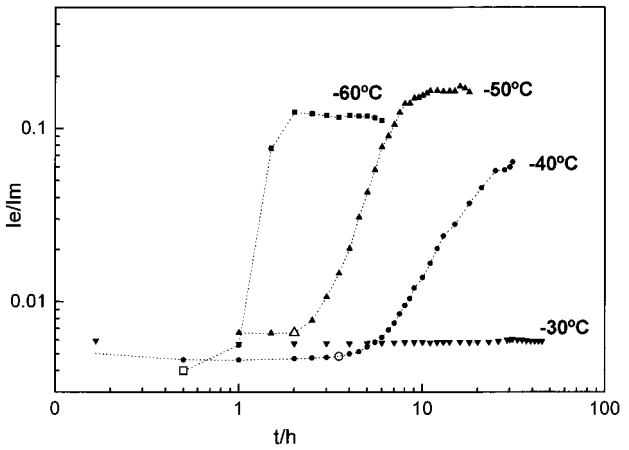

Figure 4. Average excimer (λ_{em} = 500 nm) to monomer (λ_{em} = 376 nm) fluorescence intensities ratio by excitation at λ_{exc} = 330 nm versus delay time after several instantaneous temperature quenches to −30 °C (▼), −40 °C (●), −50 °C (▲), and −60 °C (■). The frozen state duration, δ, is shown by open symbols.

longer than 100 s. At −30 °C, the I_E/I_M ratio is constant for more than 50 h, indicating that no aggregation occurs. For −40 and −50 °C three distinct regions can be observed before I_E/I_M reaches a constant value: an initial region, with duration δ, where I_E/I_M is practically constant; an intermediate region where the fluorescence intensities ratio starts increasing with time; and a final region were this ratio displays a power law dependence with time. The invariance of I_E/I_M at longer times is due to precipitation. At −60 °C the initial stage is very short, and the other two stages are too fast to be accurately followed.

The initial region corresponds to a frozen state, attributed to viscoelastic effects. Tanaka[27] found a similar frozen state during the coarsening of a polystyrene solution in diethylmalonate, attributed to the slow dynamics of the polymer-rich, viscoelastic phase. Muthukumar[34] has also observed a frozen state in the demixing of polymer blends, when an entropic barrier exists for chains transport across the interface. Viscoelastic effects are significant when the kinetic energy of Brownian motion of particles (globules and clusters) is higher than the attractive energy between them, leading to a collision contact time lower than the critical time necessary to form a stable association. This time depends on the formation of interchain entanglements. As the poly(ϵ-caprolactone) chain has a molecular weight of M_w = 20 000, higher than its critical molecular weight of entanglements, $M_e \sim 5000$, this chain should display viscoelastic effects. The M_e value was considered identical to the poly(ethylene oxide) value since both chains have a similar structure and flexibility.[35] For shallow quenches the attraction energy between particles is relatively small and their kinetic energy high, preventing association during long times. For deeper temperature quenches the kinetic energy decreases and the attraction between particles increases, favoring coalescence. This results in a decrease of the frozen state duration, δ, from 3.5 h at −40 °C to some minutes at −60 °C.

After the frozen state, the clusters reach dimensions for which viscoelastic effects are much smaller. According to Allegra,[28] clusters of flexible chains should have larger sizes than single chain globules. Viscoelastic effects should then decrease with chain incorporation.

The increase of I_E/I_M with time (Figure 4) reflects the clusters growth due to the contribution of intermolecular excimers.

In a homogeneous concentrated pyrene solution the I_E/I_M ratio is given by[32]

$$\frac{I_E}{I_M} = \frac{k_{fE}}{k_{fM}} \frac{k_1 c}{k_E + k_{-1}} \tag{1}$$

where k_{fE} and k_{fM} are the radiative rate constants for the excimer and the monomer emissions; k_E is the intrinsic lifetime of the excimer; k_1 and k_{-1} are the excimer formation and dissociation rate constants; and c is the pyrene concentration. Since aggregates with more than one chain form intermolecular excimers, I_E/I_M should be proportional to the aggregation number (N_{agg}):

$$\frac{I_E}{I_M} \propto N_{agg} \tag{2}$$

If the aggregates average density was considered invariant with size, the aggregation number, N_{agg}, would be proportional to the third power of the radius.

$$N_{agg} \propto R^3 \tag{3}$$

This assumption is reasonable because quenching temperatures are much lower than the coil−globule transition temperature, and high-density aggregates should be formed.

As the solution should have a distribution of aggregates of different sizes, the fluorescence intensity ratio should be averaged by the fraction of aggregates, $f_i = n_i/n$, with aggregation number, N^i_{agg}, giving

$$\frac{I_E}{I_M} = \sum_i \frac{n_i}{n} \frac{I_{Ei}}{I_{Mi}} \propto \sum_i \frac{n_i}{n} R_i^3 = \bar{R}^3 \tag{4}$$

where n_i is the number density of aggregates of type i, n is the total number of aggregates, and

$$\bar{R}^3 = \frac{1}{n} \sum_i n_i R_i^3 \tag{5}$$

Note that these average values are different from the gyration and hydrodynamic radius calculated from static or dynamic light scattering measurements, respectively.[36] The average radius of the aggregates scales with time as $\bar{R} \propto t^{\alpha}$, the exponent α being dependent on the growing mechanism.[9,10] Then, the excimer-to-monomer fluorescence intensities ratio should scale with time as

$$\frac{I_E}{I_M} \propto t^{\beta}$$

with $\beta = 3\alpha$.

After the frozen region aggregates start growing, and the fluorescence intensity at each time includes the contributions of both the remaining globules and aggregates. As the I_E/I_M value for intramolecular processes is independent of the amount of absorbed light, globules contribution to the fluorescence ratio stays constant in time. Then, the aggregates intermolecular contribution to fluorescence intensities ratio is simply given by the

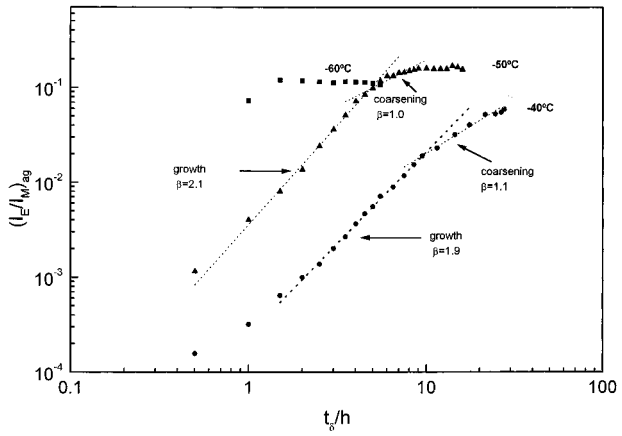

Figure 5. Aggregates averaged excimer (λ_{em} = 500 nm) to monomer (λ_{em} = 376 nm) fluorescence intensities ratios by excitation at λ_{exc} = 330 nm versus growing time, t_δ, after instantaneous temperature quenches to −40 °C (●), −50 °C (▲), and −60 °C (■).

difference between the absolute value at a given time, $(I_E/I_M)_t$, and the frozen state value, $(I_E/I_M)_\delta$, where intermolecular contribution is negligible.

Figure 5 shows a log−log plot of the fluorescence intensity ratio attributed to the aggregates, $(I_E/I_M)_{agg} = (I_E/I_M)_t - (I_E/I_M)_\delta$, as a function of growing time, $t_\delta = t - \delta$, for quenches to −40, −50, and −60 °C. The plots show two distinct linear regions before precipitation: an initial fast growth with slopes $\beta = 1.9$ (−40 °C) and $\beta = 2.1$ (−50 °C), followed by a slower one with $\beta = 1.1$ (−40 °C) and $\beta = 1.0$ (−50 °C). The whole process is too fast at −60 °C to allow accurate slopes determination.

The growth process starts when growing clusters of several chains are formed. Note that although keeping their average density constant, larger particles should show larger density gradients, having denser centers and smoothers shells. As a consequence, aggregates can grow by incorporation of globular chains, since viscoelastic effects between cluster and globules should be much smaller than among globules. This is once more in accordance with the Raos and Allegra[28] prediction that clusters have larger sizes than single chain globules, for flexible chains. When the growth is controlled by diffusion, a value of $\alpha = 0.5$ ($\beta = 1.5$) is theoretically predicted.[37] The experimental value of $\beta = 2.0 \pm 0.1$, obtained for both −40 and −50 °C, indicates that the growth process is not completely diffusion-controlled. Indeed, viscoelastic effects can increase the value of β from 1.5 to 3.0, when the growth is controlled by the coalescence on the encounter.[11] Inspection of Figure 5 shows that the initial stage duration is longer at −40 °C than at −50 °C. This is also a consequence of viscoelastic effects that are more significant at higher temperatures and retard the beginning of the growth process. During this stage the number of globules in the majority phase decreases substantially, inducing the appearance of coarsening among large aggregates for longer times.

In the coarsening stage the number of aggregates decreases in time while the average radius increases with exponent $\alpha = {}^1/_3$ for diffusion-controlled processes.[12,13] The observed value of $\beta = 1.0 \pm 0.1$ for both temperatures, corresponding to $\alpha = {}^1/_3$, indicates that coarsening is diffusion-controlled. Values of $\alpha = 1.0$ were observed on the spinodal decomposition of polymer solutions and blends when hydrodynamic flow effects

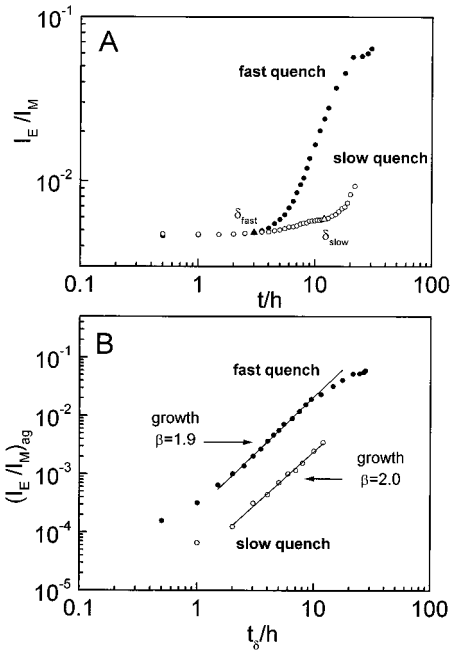

Figure 6. Variation of the averaged excimer (λ_{em} = 500 nm) to monomer (λ_{em} = 376 nm) fluorescence intensities ratio (λ_{exc} = 330 nm) versus time after an instantaneous (●) and a 25 min (○) quench to −40 °C: (A**)** absolute values of I_E/I_M versus delay time; (B**)** aggregates contribution to I_E/I_M versus growing time. (△) Values corresponding to the frozen state duration.

were important.[18,19] These effects are negligible in our case since the solution is very diluted and the interactions among aggregates are insignificant.

Figure 6 shows the average excimer-to-monomer fluorescence intensities ratio for two different quenches to −40 °C: an instantaneous, where the cell was introduced inside a cryostat already stabilized at −40 °C, and a slow one, in which the cell was inserted at room temperature and took 25 min to reach the final temperature of −40 °C.

An identical but longer initial period (frozen state) is observed for the slow quench (see Figure 6A). The precise evaluation of the beginning of the growth process, δ, is difficult to determine. In the instantaneous quench experiment, polymer chains at −40 °C can encounter and form small clusters during the process of globulization. Contrarily, during the temperature lowering in the slow quench, equilibrium compact globules are formed before temperature reaches the coexistence curve, as the coil−globule transition temperature is crossed first. When the two-phase region of the phase diagram is finally reached, the solution is composed of compact globules that can collide many times before coalescence and form clusters. The frozen stage becomes longer. However, the growth stage should proceed by the same mechanism in both quenches, which was confirmed by the value of $\beta = 2.0$ obtained for the slow quench. The uncertainty in δ is not a limitation, because the slope varies very slightly with δ. Values of $\beta = 2.0 \pm 0.1$ were obtained with δ changing from 5.5 to 12 h.

Figure 7 shows the fluctuations in the excimer intensities for a slow quench to −40 °C.

The plot shows some differences compared to the fast quench (see Figure 3A), namely in the final stage, when isolated aggregates are detected in the slow but not in the instantaneous quench. The picks width at half-maximum intensity is approximately constant for the

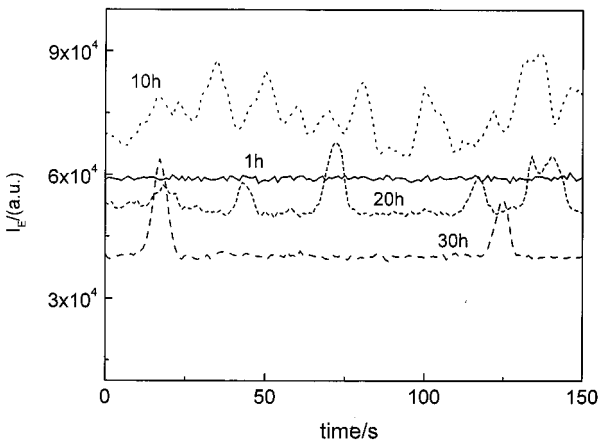

Figure 7. Excimer fluorescence (λ_{em} = 500 nm) intensity by excitation at λ_{exc} = 330 nm versus time for several delay times after a 25 min quench to −40 °C.

slow quench, therefore leading to the conclusion that in the slow quench the number density of growing clusters is lower and that the polydispersivity of the final aggregates is smaller.

In conclusion, the viscoelastic effects are very important on the phase demixing of diluted polymer solutions, slowing down the whole process. They are more significant at short delay times and when slower temperature quenches are used.

4. Conclusion

The aggregation of a very diluted poly(ϵ-caprolactone) solution in THF was studied after several temperature quenches by fluorescence. Three kinetic regimes were observed before precipitation, with durations dependent on the quenching conditions. These regimes resemble the nucleation and growth mechanism (NG) described for polymer demixing in the metastable region of the phase diagram. However, our results show that for very diluted solutions the demixing is different from the classical NG mechanism. In the NG mechanism, clusters smaller than critical droplets of micrometer sizes are unstable, being continuously formed and destructed until they reach their critical dimension. In our case, the growing clusters are small aggregates whose growth is retarded by viscoelastic effects. There is no sudden formation of micrometer size droplets, as evidenced by the continuous increase of I_E/I_M with time.

These results are not in contradiction with the former studies of spinodal demixing under critical and near-critical conditions, where the process is considered instantaneous. Under critical and near-critical conditions, quenching temperature is not far from the coil−globule transition temperature. In that case, the formed globules are loose and viscoelastic effects are negligible. An instantaneous growth is then expected. For very diluted solutions of small flexible chains, where the coil−globule transition and phase demixing temperatures are very different from each other, viscoelastic effects are dominant, and the whole process is retarded. Viscoelastic effects lose importance with domains size growth, and they are just dominant during the frozen state. The demixing is accelerated by deeper temperature quenches and retarded by slower rates of quenching.

Fluorescence was proved to be an excellent tool for phase demixing studies. It allows determination of kinetic laws during phase demixing, even in the problematic situation of very diluted solutions of small polymer chains, which are still not possible to study by other techniques.

Acknowledgment. The authors thank Prof. M. A. Winnik for generously supplying the polymer sample. This work was supported by the "Fundação para a Ciência e Tecnologia" (FCT) under the project PRAXIS XXI72/2.1/QUI/236/94. S. Piçarra acknowledges PRAXIS XXI for the PhD grant (GGPXXI/BD/2979/96).

References and Notes

(1) Imre, A.; Van Hook, W. A. *J. Phys. Chem. Ref. Data* **1996**, *25*, 637 and references therein.
(2) Sanchez, I. C. In *Encyclopedia Phys. Sci. Tech.*; Academic Press: New York, 1987; Vol. II.
(3) Gunton, J. D.; San Miguel, M.; Sahni, P. In *Phase Transition and Critical Phenomena*; Domb, C., Lebowitz, J. L., Eds.; Academic Press: London, 1983; Vol. 8.
(4) Elias, H.-G In *An Introduction to Polymer Science*; VCH: New York, 1997.
(5) Grosberg, A. Yu.; Khoklov, A. R. In *Statistical Physics of Macromolecules*; AIP Press: New York, 1994.
(6) Szydlowski, J.; Van Hook, W. A. *Macromolecules* **1998**, *31*, 3255.
(7) Lal, J.; Bansil, R. *Macromolecules* **1991**, *24*, 290.
(8) (a) Haas, C. K.; Torkelson, J. M. *Phys. Rev. Lett.* **1995**, *75*, 3134. (b) Song, S.-W.; Torkelson, J. M. *Macromolecules* **1994**, *27*, 6389.
(9) Krishnamurthy, S.; Bansil, R. *Phys. Rev. Lett.* **1983**, *50*, 2010.
(10) Tokuyama, M.; Enomoto, Y. *Phys. Rev. Lett.* **1992**, *69*, 312.
(11) Sato, H.; Kuwahara, N.; Kubota, K. *Phys Rev. E* **1994**, *50*, 1752.
(12) Lifshitz, I. M.; Slyozov, V. V. *J. Phys. Chem. Solids* **1961**, *19*, 35.
(13) Binder, K.; Stauffer, D. *Phys. Rev. Lett.* **1974**, *33*, 1006.
(14) Cahn, J. W.; Hilliard, J. E. *J. Chem. Phys.* **1958**, *28*, 258.
(15) de Gennes, P.-G. *J. Chem. Phys.* **1980**, *72*, 4756.
(16) Pincus, P. *J. Chem. Phys.* **1981**, *75*, 1996.
(17) Binder, K. *J. Chem. Phys.* **1983**, *79*, 6385.
(18) (a) Kawasaki, K.; Ohta, T. *Prog. Theor. Phys.* **1978**, *59*, 362. (b) Kawasaki, K. *Phys. Rev. A* **1991**, *44*, 817.
(19) Siggia, E. D. *Phys. Rev. A.* **1979**, *20*, 595.
(20) Velasco, E.; Toxvaerd, S. *Phys. Rev. Lett.* **1993**, *71*, 388.
(21) Glotzer, S. C.; Gyure, M. F.; Sciortino, F.; Coniglio, A.; Stanley, H. E. *Phys. Rev. E* **1994**, *49*, 247.
(22) Grosberg, A. Yu.; Kuznetsov, D. V. *Macromolecules* **1993**, *26*, 4249.
(23) Ivanov, V. A.; Paul, W.; Binder, K. *J. Chem. Phys.* **1998**, *109*, 5659.
(24) Noguchi, H.; Yoshikawa, K. *J. Chem. Phys.* **1998**, *109*, 5070.
(25) Chu, B. *Appl. Opt.* **1997**, *36*, 7650.
(26) Raos, G.; Allegra, G. *J. Chem. Phys.* **1997**, *107*, 6479.
(27) (a) Tanaka, H. *Phys. Rev. Lett.* **1993**, *71*, 3158. (b) *Macromolecules* **1992**, *25*, 6377.
(28) (a) Raos, G.; Allegra, G. *Macromolecules* **1996**, *29*, 8565. (b) *Macromolecules* **1996**, *29*, 6663.
(29) Piçarra, S.; Gomes, P. T.; Martinho, J. M. G. *Macromolecules* **2000**, 33, 3947.
(30) Sosnowski, S.; Slomkowski, S.; Penczek, S. *Makromol. Chem.* **1991**, *192*, 1457.
(31) Winnik, M. A.; Redpath, A. E. C.; Paton, K.; Jarda, D. *Polymer* **1984**, *25*, 91.
(32) Birks, J. B. *Photophysics of Aromatic Molecules*; Wiley-Interscience: London, 1970; p 19.
(33) Pasternack, R. F.; Collings, P. J. *Science* **1995**, *269*, 935.
(34) Kotnis, M. A.; Muthukumar, M. *Macromolecules* **1992**, *25*, 1716.
(35) Wool, R. P. *Polymer Interfaces, Structure and Strength*; Hanser Publishers: New York, 1993.
(36) Chu, B. *Laser Light Scattering: Basic Principles and Practice*, 2nd ed.; Academic Press: New York, 1991.
(37) Cummig, A.; Wiltzius, P.; Bates, F. S. *Phys. Rev. Lett.* **1990**, *65*, 863.

MA001231T